Hybrid Microgels with Thermo-Tunable Elasticity for Controllable Cell Confinement

*Sebastian Hackelbusch, Torsten Rossow, Dirk Steinhilber, David A. Weitz, and Sebastian Seiffert**

Stimuli-responsive hydrogels are able to change their physical properties such as their elastic moduli in response to changes in their environment. If biocompatible polymers are used to prepare such materials and if living cells are encapsulated within these networks, their switchability allows the cell–matrix interactions to be investigated with unprecedented consistency. In this paper, thermo-responsive macro- and microscopic hydrogels are presented based on azide-functionalized copolymers of poly(*N*-(2-hydroxypropyl)-methacrylamide) and poly(hydroxyethyl methacrylate) grafted with poly(*N*-isopropylacrylamide) side chains. Crosslinking of these comb polymers is realized by bio-orthogonal strain-promoted azide–alkyne cycloaddition with cyclooctyne-functionalized poly(ethylene glycol). The resulting hybrid hydrogels exhibit thermo-tunable elasticity tailored by the polymer chain length and grafting density. This bio-orthogonal polymer crosslinking strategy is combined with droplet-based microfluidics to encapsulate living cells into stimuli-responsive microgels, proving them to be a suitable platform for future systematic stem-cell research.

1. Introduction

Stimuli-responsive hydrogels are three-dimensionally crosslinked polymer networks swollen with water, exhibiting physical properties that selectively change upon variation of environmental parameters.[1] These materials have promising potential to serve as sensitive scaffolds in regenerative medicine[2,3] and tissue engineering[4–6] due to their controllable mechanical properties, which are similar to those of soft tissue. In a particularly promising class of application, stimuli-responsive hydrogels are employed to investigate the influence of external mechanical constraint on cells, including cell viability,[7,8] morphogenesis,[9,10] and differentiation.[11,12] For example, photodegradable poly(ethylene glycol) hydrogels have been demonstrated to induce stem-cell differentiation as a result of gradually decreasing gel rigidity.[13] In an opposite approach, stem-cell-laden hyaluronic acid gels were additionally photocrosslinked, thereby increasing their mechanical rigidity and triggering the stem cell differentiation to change from osteogenesis to adipogenesis.[14] However, both such photo-induced gel degradation and gel stiffening is irreversible and proceeds in just one direction. To overcome this limitation, hydrogels based on polymers that exhibit a lower critical solution temperature (LCST) in water can be used to enable selective and reversible bidirectional switching between different states.[15–17] In a recent seminal work, a hydrogel based on thermo-responsive poly(*N*-isopropylacrylamide) (PNIPAAm) was used for stem-cell encapsulation.[18] This polymer changes its polymer–solvent interaction from hydrophilic to hydrophobic at an LCST of ≈34 °C,[19] entailing dramatic deswelling of the gel and an increase of the gel elastic modulus. When mesenchymal stem cells are implanted into this hydrogel, increase of the temperature to 37 °C causes hydrogel-collapse inducing stem-cell differentiation into tooth tissue, analogous to mesenchymal condensation.[20] However, in this approach, the hydrogel preparation occurred by free-radical polymerization, thus prohibiting the encapsulation of cells during the process of hydrogel formation due to proven cytotoxicity of the free radicals.[21,22] Additionally, all the aforementioned approaches of tunable-gel fabrication focus on preparing macrogels rather than gels with microscopic dimensions. This is unfortunate, because hydrogel particles with micrometer-scale dimensions, often referred to as microgels, are particularly useful to study stem cell fate, because such microgels are easy to manipulate with micropipettes and microsyringes, and because they impart just small diffusion barriers to cellular nutrients and metabolites.[23,24] To encapsulate living cells into microgel particles, the technique of droplet-based microfluidics has recently been combined with bioorthogonal and cytocompatible crosslinking of macromolecular precursors.[25,26] With this approach, however, no reversibly responsive cell-laden microgels have

S. Hackelbusch, Dr. T. Rossow, Prof. S. Seiffert
Freie Universität Berlin
Institute of Chemistry and Biochemistry
Takustr. 3, D-14195 Berlin, Germany
E-mail: seiffert@chemie.fu-berlin.de
Dr. T. Rossow, Prof. S. Seiffert
Helmholtz-Zentrum Berlin
Soft Matter and Functional Materials
Hahn-Meitner-Platz 1, D-14109 Berlin, Germany
Dr. T. Rossow, Prof. S. Seiffert
Helmholtz Virtual Institute "Multifunctional Materials for Medicine"
Kantstr. 55, D-14513 Teltow, Germany
Dr. D. Steinhilber, Prof. D. A. Weitz
Harvard University
School of Engineering and Applied Science
29 Oxford Street, Cambridge, Massachusetts 02138, U.S.A.

DOI: 10.1002/adhm.201500359

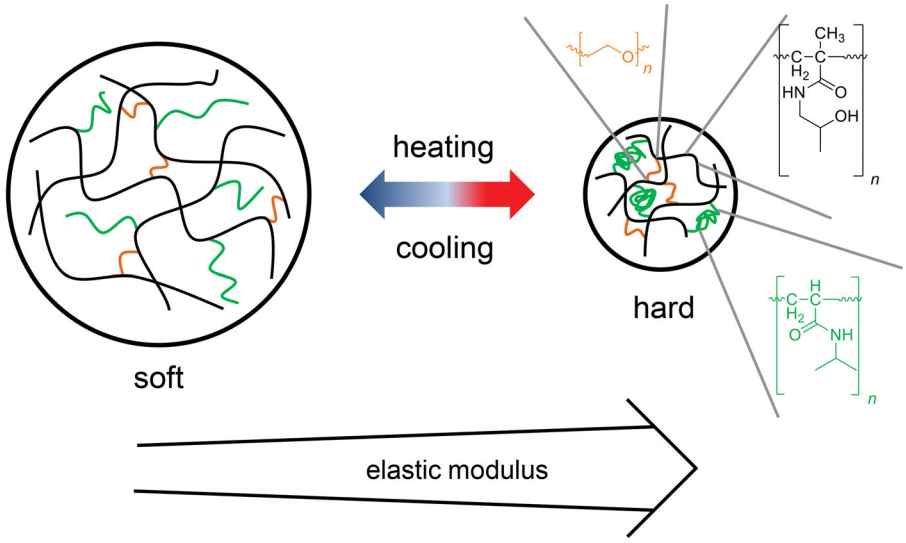

Figure 1. Schematic of thermo-responsive hybrid microgel particles composed of poly(*N*-(2-hydroxypropyl)-methacrylamide) (PHPMA) covalently crosslinked with poly(ethylene glycol) (PEG) and additionally grafted with poly(*N*-isopropylacrylamide) (PNIPAAm). The microgels contract upon heating due to formation of supramolecular crosslinking nodes composed of collapsed PNIPAAm interchain clusters, entailing a reversible increase of the microgel elastic moduli.

been prepared yet. Such materials could be exceptionally useful for serving as scaffolds to investigate mechanotransduction,[27] because they would combine all the above advantages that have only been realized separate from one another to date.

In this paper, we present thermo-responsive hybrid microgels based on copolymers of poly(*N*-(2-hydroxypropyl)-methacrylamide) (PHPMA) and poly(hydroxyethyl methacrylate) (PHEMA) that are side-chain functionalized with dangling PNIPAAm chains and that are covalently crosslinked by poly(ethylene glycol) (PEG) strands, as sketched in **Figure 1**. We employ the technique of strain-promoted azide–alkyne cycloaddition (SPAAC) as a mild crosslinking method and combine this approach with droplet-based microfluidics to encapsulate living mammalian cells into the resulting thermo-responsive hybrid microgels. Upon change of temperature, these hybrid microgels can reversibly expel or take up water, entailing a reversible change of their elastic modulus, as also illustrated in Figure 1. Thus, by such variation of the microgel incubation temperature, along with previous variation of the concentration and molecular weight of the PNIPAAm side chains within the microgels, the mechanical properties of the microgels can be tuned gradually in a prescribed range of microgel elasticity and degree of swelling. This elastic switchability makes this microgel construction kit promising to act as a versatile material platform to investigate cell mechanotransduction with unprecedented consistency.

2. Results and Discussion

Our approach to form thermo-responsive hybrid microgels is based on copolymers of PHPMA that are side-chain functionalized with pendant thermo-responsive PNIPAAm chains. PHPMA can be copolymerized with a variety of comonomers by free-radical copolymerization to subsequently attach functional groups to the polymer chain. We follow this concept and copolymerize (*N*-2-hydroxypropyl)-methyacrylamide (HPMA) with 5 mol% of 2-hydroxyethyl methacrylate (HEMA), using ^{1}H-NMR spectroscopy to ensure that the anticipated content of comonomer is indeed incorporated in the product. The terminal hydroxy groups of the HEMA moieties are then converted to azides in a subsequent two-step protocol. In the first step, the primary hydroxy groups are converted to mesylates. In the second step, a nucleophilic substitution with sodium azide yields an azide-functionalized PHPMA copolymer, as shown in **Scheme 1**A. After this reaction, mesyl signals can no longer be observed in the ^{1}H-NMR spectrum, but instead, a characteristic azide band at ~2100 cm^{-1} is detected by IR spectroscopy in the final product, indicating complete conversion of the mesyl groups to azide functionalities, whereas this reaction protocol does not yield PHPMA-azide when a PHPMA homopolymer is used as substrate.

To couple PNIPAAm to the azide-functionalized PHPMA chains, it is end-capped with cyclooctyne motifs. For this purpose, we first prepare two sets of amine-terminated PNIPAAm with number-average molecular weights of 10 000 g mol^{-1} and 25 000 g mol^{-1} (both polystyrene-analog) by free-radical polymerization of *N*-isopropyl acrylamide (NIPAAm) in the presence of 2-aminoethanethiol (AET), which acts as a radical scavenger, thereby creating an amine terminus on each chain. The amine-terminated PNIPAAm chains are then end-functionalized with bicyclo[6.1.0]non-4-yn-9-ylmethyl (4-nitrophenyl) carbonate (BCN),[28] thereby yielding cyclooctyne-capped PNIPAAm, as shown in Scheme 1B.

The degree of functionalization of PNIPAAm with cyclooctyne caps is determined in a two-step protocol. First, we determine the functionalization of PNIPAAm with terminal amine groups by reaction of a portion of the PNIPAAM-amine with a 10-fold excess of fluorescein isothiocyanate (FITC).[29] UV/VIS spectroscopic characterization of the labeled product denotes the degree of functionalization of the PNIPAAm to be 95%. Second, we react the PNIPAAm-amine with an excess of the cyclooctyne derivative and then with FITC again. If no residual FITC absorbance can be observed in subsequent UV/VIS spectroscopy, complete conversion of the terminal amine groups to cyclooctynes is proven; this was the case for the present set of PNIPAAm polymers. Subsequently, these cyclooctyne-functionalized polymers are coupled to the azide groups of the P(HPMA-*co*-HEMA) backbone polymer by strain-promoted azide–alkyne cycloaddition (SPAAC), which was previously shown to proceed with quantitative conversion.[30]

Crosslinking of these thermo-responsive comb polymers to forming hydrogels is achieved by using 1 mol% of

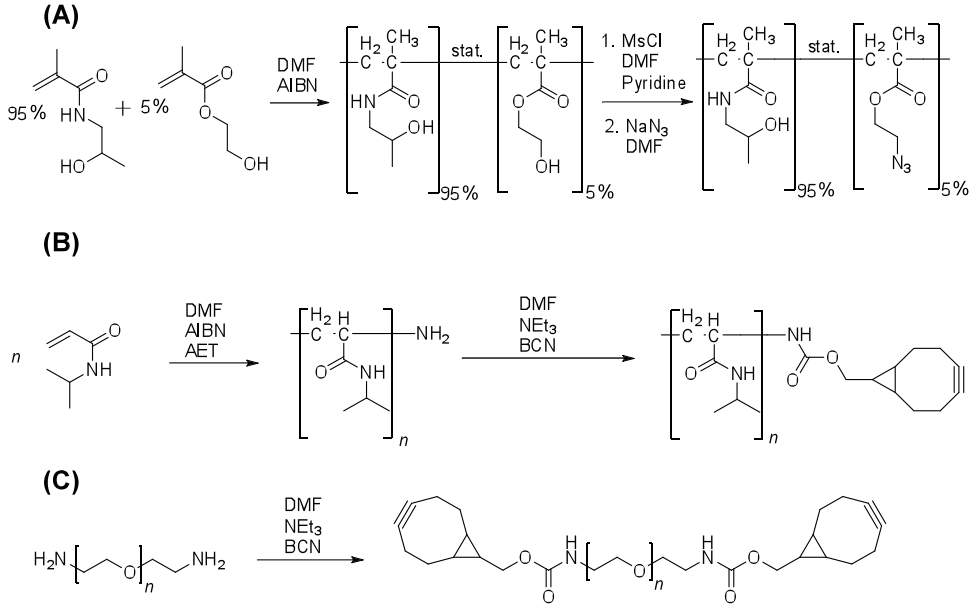

Scheme 1. Synthetic route toward azide-functionalized poly(*N*-(2-hydroxypropyl)-methacrylamide) (PHPMA) and cyclooctyne-functionalized poly(*N*-isopropylacrylamide) (PNIPAAm) and poly(ethylene glycol) (PEG).

PEG-bis(cyclooctyne) as a crosslinker in another SPAAC reaction, previously prepared by conversion of PEG-diamine with BCN, as shown in Scheme 1C. This amount of crosslinker is typical for soft hydrogels that have elastic moduli similar to that of natural tissues.[31,32] To vary the mechanical properties of the resulting hydrogels in a modular fashion, we employ PEG with different molecular weights: 1500, 6000, and 20 000 g mol^{-1}, denoted PEG_{1500}, PEG_{6000}, and $PEG_{20\,000}$. Furthermore, the degree of additional functionalization of the P(HPMA-*co*-HEMA) with PNIPAAm is chosen to be either 1 mol% or 2.5 mol%, using PNPAAm polymers with two different number-average molecular weights, 10 000 and 25 000 g mol^{-1}, denoted $PNIPAAm_{10\,000}$ and $PNIPAAm_{25\,000}$. As a result, we obtain a set of $2 \times 2 \times 3 = 12$ different polymer networks, formed with two different contents of pendant PNIPAAm, two different molecular weights of the pendant PNIPAAm, and crosslinked by PEG chains with three different molecular weights. In all cases, the overall polymer concentration is kept constant at 100 g L^{-1}.

To examine the thermo-responsiveness of the P(HPMA-*co*-HEMA) backbone polymers functionalized with either 1 or 2.5 mol% of PNIPAAm, the LCST of their aqueous solutions is estimated by temperature-dependent hydrodynamic-size estimation based upon dynamic light scattering (DLS). Upon increase of the temperature to 32 °C, the hydrodynamic diameter of both copolymers, calculated from their translational diffusion coefficients probed by DLS, increases from 38 nm at 28 °C to 284 nm at 32 °C due to formation of hydrophobic clusters in the solution. Below 28 °C and above 32 °C, the hydrodynamic diameters of the polymer coils in both samples are independent of temperature. The DLS measurements are carried out in water as well as cell medium (Dulbecco's Modified Eagles's Medium, pH 7.4), showing no significant difference in the hydrodynamic diameters, respectively. In the following, the mechanical properties of the corresponding hydrogels are investigated in cell medium at 28 °C and 32 °C, respectively.

To assess the mechanical properties of the polymer networks, the different hydrogels are probed by oscillatory shear rheology. As a basis of the rheological tests, we first probe semidilute solutions of PHPMA-*co*-PNIPAAm with 2.5 mol% functionalization of $PNIPAAm_{10\,000}$ and $PNIPAAm_{25\,000}$ at 100 g L^{-1}. At 28 °C, these samples exhibit scaling of the frequency-dependent storage and loss moduli, $G'(\omega)$ and $G''(\omega)$, close to $G' \sim \omega^2$ and $G'' \sim \omega^1$ in the range of $\omega = 0.01$–16 Hz, in agreement with the Maxwell model for viscoelastic polymer solutions. Upon increase of the temperature to 32 °C, G' and G'' intersect at frequencies in the range of 0.01–1 Hz, with G' reaching a plateau at higher frequencies, representing weak polymer gels. The values for G' and G'' measured at 32 °C are 10 times higher for $PNIPAAm_{10\,000}$ and 100 times higher for $PNIPAAm_{25\,000}$ in comparison to those measured at 28 °C, respectively. This observation can be explained by microphase separation of the PNIPAAm pendant chains within the semidilute solutions above the PNIPAAm–water LCST, which leads to formation of nanoscopic hydrophobic clusters that act as physical crosslinks. To exclude further changes of the elastic moduli of the gels at higher temperatures, we probe a sample at 32 and 37 °C, respectively, observing no further effect.

Upon mixing the PHPMA-azide polymer solutions with PEG-bis(cyclooctyne) and PNIPAAm-cyclooctyne, thermo-sensitive hydrogels are prepared in situ. All these gels exhibit almost frequency-independent plateaus in G' ($\omega = 0.01$–16 Hz) at both 28 °C and 32 °C, but these plateau moduli show a strong temperature dependence, as compiled in **Table 1**A and 1B. At 28 °C, use of a longer crosslinker chain length results in higher elastic moduli, along with enhanced crosslinking efficiencies, ν_{eff}, representing the relation of the concentration of crosslinks in the sample, ν, to the maximum possible concentration of crosslinks,

Table 1. Elastic moduli of thermo-responsive PEG–PHPMA–PNIPAAm hydrogels containing A) 1 mol% and B) 2.5 mol% of pendant graft PNIPAAm, along with a constant amount of PEG crosslinker (1 mol%), as determined by oscillatory shear rheology at 28 °C and 32 °C, respectively. The values of G' are estimated at the frequency-dependent minimum of G'', corresponding to a minimal loss tangent. The polymer-crosslinking efficiency, ν_{eff}, of the hydrogels can be calculated by $\nu_{eff} = \nu_{nodes}/\nu_{theo}$, where ν_{theo} is the theoretical concentration of crosslinking junctions in each sample, corresponding to its concentration (mol L^{-1}) of cyclooctyne moities, whereas ν_{nodes} corresponds to the actual concentration of the elastically effective crosslinks in the sample. We use the phantom network model to estimate the latter parameter from the plateau values of the elastic moduli of the different hydrogels, $\nu_{nodes} = 2/3 \cdot \nu_{strands} = 2/3 \cdot G'/(ART\varphi_M)$, with R the gas constant, φ_M the mass fraction of polymer ($\varphi_M = m_{polymer}/(m_{polymer} + m_{solvent})$), and T the temperature; A is a structure fracture that equals $1 - 2/f$, with f the functionality of the crosslinks, which we assign to be 3. The factor 2/3 is attributed to the geometry of the network: each junction is connected to three network strands, whereas each strand has two junctions at its two ends.[43]

(A)

1% PNIPAAm	28 °C				32 °C	
	$PNIPAAm_{10\,000}$		$PNIPAAm_{25\,000}$		$PNIPAAm_{10\,000}$	$PNIPAAm_{25\,000}$
	G' [Pa]	ν_{eff} [%]	G' [Pa]	ν_{eff} [%]	G' [Pa]	G' [Pa]
PEG_{1500}	8	0.9	3	0.4	64	93
PEG_{6000}	201	26.8	16	1.6	400	176
$PEG_{20\,000}$	383	74.8	482	110.5	594	706

(B)

2.5% PNIPAAm	28 °C				32 °C	
	$PNIPAAm_{10\,000}$		$PNIPAAm_{25\,000}$		$PNIPAAm_{10\,000}$	$PNIPAAm_{25\,000}$
	G' [Pa]	ν_{eff} [%]	G' [Pa]	ν_{eff} [%]	G' [Pa]	G' [Pa]
PEG_{1500}	4	0.7	0.1	0.03	30	81
PEG_{6000}	13	2.6	32	9.2	71	754
$PEG_{20\,000}$	288	75.2	52	18.1	419	125

ν_{theo}. This finding can be ascribed to the small hydrodynamic diameters of the crosslinking PEG_{1500} and PEG_{6000} polymers, which are determined to be 2.1 nm and 4.5 nm by DLS, respectively. Elastically effective network junction nodes are formed only when both cyclooctyne moieties of a given PEG crosslinker react with azide moieties of two different PHPMA chains. Hence, for the PEG_{1500} and PEG_{6000} linkers to constitute such effective network junctions, two PHPMA chains need to be in close proximity when reacting with the PEG, which is, however, not likely to occur at an overall polymer concentration of 100 g L^{-1}. As a result, mostly dangling chains and loops are formed in case of PEG_{1500} and PEG_{6000}, and these network defects do not contribute to the elastic energy storage.[33] By contrast, when $PEG_{20\,000}$ is used for the crosslinking, which exhibits a hydrodynamic diameter of 12.7 nm, interchain crosslinking occurs with high efficiency that even exceeds 100% (Table 1A). This finding can be attributed to trapped chain entanglements inside the resulting polymer networks that add further elastically effective network-crosslinking nodes to the junctions formed by the covalent chain crosslinking.[34,35]

The thermo-responsive reversible switchibility of the elastic moduli of the different hydrogels is more distinct for samples with small low-temperature moduli and small covalent crosslinking efficiencies than for samples with large low-temperature moduli and large covalent crosslinking efficiencies, as represented by the differences between the respective moduli at 28 °C and 32 °C in Table 1A and 1B. We relate this finding to the content and chain length of pendant PNIPAAm within the different gels. The average distance between the pendant PNIPAAm chains in the hydrogels, $\delta_{PNIPAAm}$, can be calculated from their molar concentrations in the gel by $\delta_{PNIPAAm} = (c_{PNIPAAm} N_A)^{-1/3}$, with $c_{PNIPAAm}$ the concentration of PNIPAAm in the sample and N_A the Avogadro constant. These distances are in the range of 73 to 95 nm for the different hydrogels studied, significantly exceeding the hydrodynamic diameters of $PNIPAAm_{10\,000}$ (7.4 nm) and $PNIPAAm_{25\,000}$ (10.1 nm), as determined by DLS. As a result, an effective formation of hydrophobic clusters during the thermo-induced collapse of these PNIPAAm chains requires a minimum flexibility of the polymer scaffold to which they are bound to allow them to reach one another. For quantification, we determine the root-mean-square maximum excursion of the PNIPAAm chains in the different hydrogels, $\langle x^2 \rangle^{1/2}$, on basis of Weitz' and Mason's microrheology concept in the long-term limit of a rubbery-elastic medium: $\langle x^2 \rangle = kT/(\pi G' d_{PNIPAAm})$, with T the temperature, k the Boltzmann constant, G' the plateau value of the elastic modulus, and $d_{PNIPAAm}$ the hydrodynamic diameter of the respective PNIPAAm chains.[36,37] In the case of the systems that are efficiently covalently crosslinked but show little thermo-responsiveness, this maximum excursion is in the range of just 19 to 52 nm, which does not allow these chains to reach one another to form hydrophobic clusters upon collapse above their LCST. By contrast, the systems that are weakly covalently crosslinked but exhibit a pronounced thermo-responsiveness have PNIPAAm-chain maximum excursions in the range of 75 to 1334 nm, which enables the PNIPAAm chains to reach each other and form hydrophobic clusters above the LCST.

The formation of the covalent crosslinking contribution of the present set of gels occurs in a controlled polymer-analogous reaction; this can be expected to yield more homogenous polymer networks than those usually formed by uncontrolled free-radical polymerization.[38,39] To check whether such

favorable homogeneity is found in the present class of gels, we probe a hydrogel composed of PHPMA crosslinked with 1 mol% of PEG_{6000} crosslinker without any additional pendant PNIPAAm at a concentration of 67 g L^{-1} by static light scattering followed by data evaluation according to the Debye–Bueche method.[40,41] In this approach, it is assumed that the scattering intensity of a gel sums up of thermal concentration fluctuations (ergodic contribution) and static spatial inhomogeneities resulting from the crosslinking (nonergodic contribution). To quantify the latter, it is presumed that the thermal fluctuations are identical to those in an uncrosslinked semidilute solution of the same polymer. Hence, the excess light scattering intensity of a polymer gel can be determined from the difference of the angle-resolved scattering between a crosslinked and an uncrosslinked sample.[42] We estimate this for the 67 g L^{-1} crosslinked sample and an uncrosslinked sample that contains unfunctionalized non-crosslinking PEG_{6000}. Subsequent data evaluation by the Debye–Bueche method yields the root-mean-square spatial refractive index fluctuation, which can be converted into the spatial concentration fluctuation in the polymer network if the refractive index increment of the constituent polymer is known.[40,43] For the investigated hydrogel, we determine a percentage concentration fluctuation of only (3×10^{-7})%. This estimate supports the hypothesis that our PHPMA-based hydrogels are very homogeneous.

To prepare monodisperse microscopic gel particles from the present class of polymers, we apply the technique of droplet-based microfluidics.[25,44] This technique uses emulsion droplets as templates for particle fabrication, with exquisite control on the droplet size, dispersity, and shape. Subsequent droplet gelation yields a set of microgels that retain the pre-microgel droplet monodispersity, shape, and size. We use poly(dimethylsiloxane) (PDMS) microchannels with two sequential cross-junctions and three separate inlets for the inner fluid phases, fabricated by soft lithography.[44] In the left inlet, an aqueous mixture of cyclooctyne-functionalized PNIPAAm and PEG is injected, whereas in the right inlet, an aqueous solution of azide-functionalized PHPMA is injected. The middle inlet is used for either water as a blocker phase or for cell-containing media to achieve cell encapsulation, as shown in **Figure 2**A. After their injection, these three fluids meet at the first cross-junction and form a laminar coflowing stream in the microchannel. In the second junction, periodic break-up of the stream is induced by flow-focusing with a fourth fluid, which is immiscible paraffin oil. By this mechanism, uniform pre-microgel droplets with a size of 140 µm and an overall polymer concentration of 100 g L^{-1} are formed, as depicted in Figure 2B. Gelation occurs by mixing of the three liquids inside the droplets, leading to formation of microgel particles, as shown in Figure 2C. We prepare microgels with two different compositions: PHPMA with 1 mol% of $PNIPAAm_{25\,000}$ and PHPMA with 2.5 mol% of $PNIPAAm_{25\,000}$, both crosslinked by 1 mol% PEG_{6000}.

A check for comparability of the mechanical properties of the macro- and microscopic gels prepared by the different preceding approaches can be performed by determining their equilibrium degrees of swelling. This is done using either model microgels without any cell load or a macroscopic gel specimen with the same composition as the microgels. After producing and washing these micro- and macrogels, we store them in an aqueous phase for a period of several hours to achieve equilibrium swelling, respectively. The swollen microgel particle are subsequently densified by centrifugation at 600 RCF for 10 min. Upon removal of the supernatant swelling agent, the remaining particle suspension is a random close packing of spheres with a space filling of 64%. The degree of microgel swelling, Q, can then be determined by comparing the wet and dry weight of the concentrated particle suspension, w_{wet} and w_{dry}; we calculate it as $Q = (0.64 w_{wet} - w_{dry})/w_{dry}$. The estimated degree of microgel swelling is identical to that of a corresponding macrogel sample, which indicates that the elastic moduli of these differently sized materials are comparable.

To demonstrate the cytocompatibility of our hydrogel materials, we encapsulate living cells into microgel particles formed from them, again shaped through droplet-based microfluidic templating as detailed above and as illustrated in Figure 2A. As a model cell line, we chose NIH 3T3 mouse embryonic fibroblasts. After preparation and work-up of the cell-laden microgels, one fraction of them is incubated over night at 28 °C; these microgels are crosslinked only by the covalent PEG linkers within them, but not by additional reversible crosslinking due to PNIPAAm clustering. By contrast, another microgel fraction is stored at 37 °C; these microgels exhibit both permanent crosslinking by pEG and additional reversible supramolecular crosslinking by PNIPAAm clustering. To ensure absence of

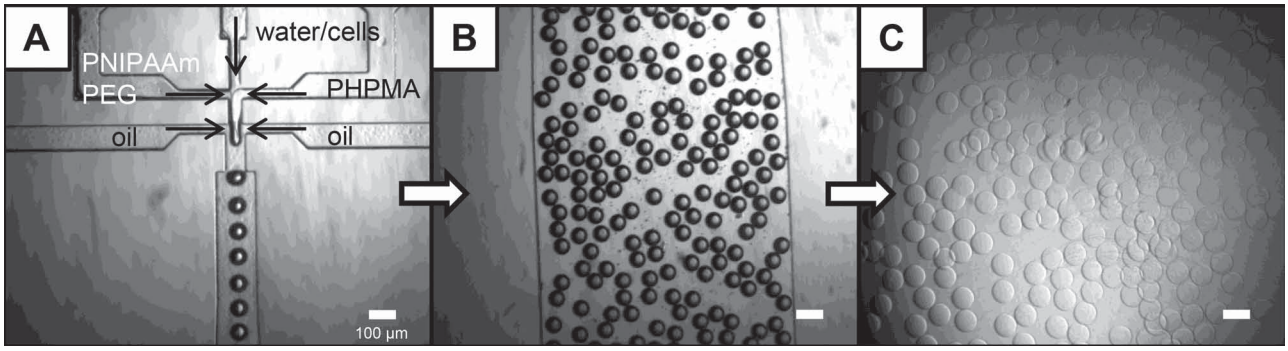

Figure 2. Fabrication of hybrid microgel particles by droplet-based microfluidics. A) Two sequential cross-junction channels serve to form monodisperse precursor droplets that consist of aqueous solutions of cyclooctyne-functionalized PEG and PNIPAAm as well as azide-functionalize PHPMA, optionally along with cells. B) Pre-microgel droplets formed from the experiment in panel (A) in a basin channel patterned downstream of the two sequential cross-junctions. C) Micrograph of swollen hybrid microgel particles formed by gelation of the pre-microgel droplets shown in panels (A,B).

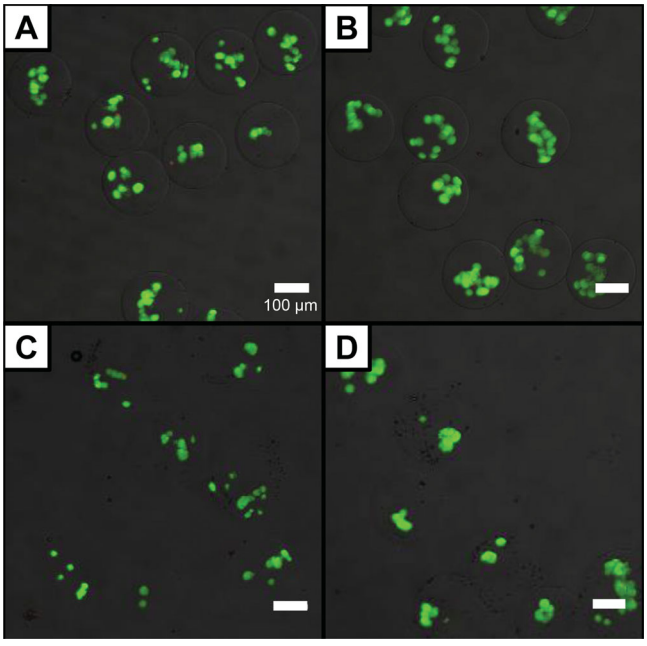

Figure 3. Optical micrographs (bright field and confocal fluorescence, overlaid) of cell-laden thermo-responsive hybrid microgels after incubation over night. Green staining denotes living cells, whereas dead cells are stained red. A,B) Microgels composed of PHPMA with 1 mol% of graft $PNIPAAm_{25\,000}$ incubated at A) 28 °C and B) 37 °C. C,D) Microgels composed of PHPMA with 2.5 mol% of graft $PNIPAAm_{25\,000}$ incubated at C) 28 °C and D) 37 °C.

inefficient cell encapsulation during the microfluidic steps, the supernatant solution that is left over after the microgel work-up is investigated to check for presence of free cells; however, none of the batches used for further investigations has shown any.

The viability of the encapsulated cells is determined by fluorescence-based live–dead assays, staining living cells green and dead cells red, as shown in **Figure 3**. In this assessment, all microgel fractions exhibit cell viabilities greater than 90% independent of the incubation temperature after one day. To further challenge the utility of the present class of microgels for cell encapsulation, we load them with bone marrow-derived stem cells, performed in similar experimental fashion. In this set of experiments, the stem cells exhibit viabilities of around 80% after 1 day of incubation at 37 °C, again determined by fluorescence-based live–dead assays. These results are a promising basis for future work on studying stem-cell differentiation and mechanotransduction that takes advantage of the ability for controlled switching of the elasticity of the extracellular environment provided by the present class of microgels.

3. Conclusion

Thermo-responsive hybrid microgels based on water-swollen networks of PHPMA–PNIPAAm comb polymers display favorable tunable mechanical properties similar to those of natural soft tissue. They can be prepared by bioorthogonal crosslinking of precursor polymers by SPAAC, allowing for the encapsulation of living cells with excellent viability retain. The elasticity of the microgels is adjustable by incubating them below and above the LCST of PNIPAAm in water: when heating the microgels to above 32 °C, the PNIPAAm side chains within them collapse and clusterize, causing contraction of the microgels and increase of their elastic moduli. In addition to this in situ effect, the modular principle of polymer gel formation allows the fundamental low-temperature elasticity of the microgels, which is caused by their permanent covalent crosslinking component, to be varied over a broad range. Together, this custom design principle and reversible switchability renders these microgels promising to serve as scaffold materials for inducing and studying stem-cell differentiation at an individual cell level. In a further perspective, additional microgel functionalization such as addition of peptide sequences as anchorage points for cells can easily be implanted by suitable further functionalization of the PHPMA backbone, again realizable by SPAAC. Moreover, a shift of the microgel LCST closer to the human body temperature can be achieved by copolymerization of the microgel-internal pendant PNIPAAm with acrylic acid.[19] These modifications further enrich the versatility and promise of the present system.

4. Experimental Section

All reagents, if not addressed differently, were purchased from Sigma-Aldrich and used without further purification. Deuterated solvents were purchased from Deutero. Dry dimethylformamide (DMF) and dry pyridine were purchased from Acros Organics. 2,2-azobis(2-methylpropionitril) (AIBN) was recrystallized from methanol. *N*-isopropylacrylamide (NIPAAm) was recrystallized from hexane. bicyclo[6.1.0]non-4-yn-9-ylmethyl (4-nitrophenyl) carbonate (BCN) was prepared according to literature procedures.[28] PEG-bis(cyclooctyne) and PNIPAAm-cyclooctyne were also prepared according to literature procedures, but with the difference of using DMF instead of chloroform.[26] Hydroxyethyl methacrylate (HEMA) and triethylamine were dried over calcium hydride and distilled prior to use. ^{1}H-NMR spectra were recorded on a Bruker AC 400 spectrometer. Infrared spectra were measured on a JASCO FT-IR spectrophotometer. Size exclusion chromatography (SEC) of PNIPAAm was carried out with a Thermo Separation Products pump P-100 equipped with a refractive index detector Shodex RI-71 and a UV-1000 UV detector. Columns of type PSS GRAM-1000/100–7µ were used, and polystyrene standards served to evaluate the molecular weight and size distribution of the polymer samples. The eluent was NMP (*N*-methylpyrrolidone) with 0.05 mol L^{-1} of lithium bromide and benzoic acid methylester as the internal standard. The measurements were performed at 70 °C. SEC of PHPMA-based copolymers was performed with an Agilent 1100 solvent delivery system with dosing pump, manual injector, and an Agilent 1100 differential refractometer. Three 30 cm columns (PSS Suprema, 5 µm particle size) were used to separate polymer samples, using water at a flow rate of 1 mL min^{-1} as the eluent and PEG standards were used as internal calibration.

(N-2-hydroxypropyl)-methyacrylamide (HPMA): 1-Aminopropan-2-ol (23.4 mL; 0.30 mol; 1 eq.) and dry triethylamine (42 mL; 0.30 mol; 1 eq.) were dissolved in dry dichloromethane (DCM) (120 mL) and cooled to 0 °C under argon atmosphere. While stirring, methacryloyl chloride (30 mL; 0.3 mol; 1 eq.) in dry DCM (60 mL) was added dropwise, and the solution was stirred over night. The solvent was removed in vacuo, and the pure product was obtained by flash column chromatography on silica gel with ethyl acetate, yielding HPMA (19.8 g; 65.3%).

^{1}H-NMR (400 MHz, $CDCl_3$, δ): 6.57 (b, 1H, -N*H*), 5.76 (s, 1H, C*H*-acrylate), 5.37 (s, 1H, C*H*-acrylate), 3.96 (m, 1H, -CH_2-C*H*OH-CH_3), 3.20 (m, 2H, -NH-CH_2-CHOH-), 1.98 (s, 3H, CH2 = CCH_3-CO-), 1.19 (d, 3H, -CHOH-CH_3) ppm.

Copolymerization of HPMA with HEMA: HPMA (5.0 g; 34.9 mmol; 1 eq.) and HEMA (0.4 mL; 3.49 mmol; 0.1 eq.) were dissolved in dry DMF, and the solution was pre-heated to 60 °C under argon atmosphere. AIBN (28.6 mg; 0.17 mmol) in DMF was added, and the solution was stirred over night at 60 °C. The resulting copolymer was isolated by precipitation, achieved by pouring the post-reaction mixture into a liter of cold diethylether, yielding P(HPMA$_{95}$-*co*-HEMA$_5$) (3.6 g; 66.4%). The comonomer ratio in the product copolymers was determined from the ^{1}H-NMR integral of the methin proton in the side group of PHPMA, -CH$_2$-C**H**OH-CH$_3$, and the integral of the two methylene protons of the hydroxyl-methylene sidegroup of PHEMA, -CH$_2$-C**H**$_2$-OH. Later on, the polymerization was repeated to produce greater amounts of P(HPMA-*co*-HEMA).

^{1}H-NMR (400 MHz, DMSO-d$_6$, δ): 7.02 (b, -N*H*), 4.83 (m, -COO-C*H*$_2$-), 4.69 (m, -CH$_2$-C*H*OH-CH$_3$), 3.88 (m, -CH$_2$-C*H*$_2$-OH), 3.66 (m, -NH-C*H*$_2$-CHOH-), 2.00–0.68 (m, polymer backbone) ppm.

SEC (PEG calibration): M_n = 15,700 g mol^{-1}, M_w = 43,900 g mol^{-1}, M_w/M_n = 2.8.

Modification of P(HPMA$_{95}$-co-HEMA$_5$) to Yield Azide-Functionalized PHPMA: P(HPMA$_{95}$-*co*-HEMA$_5$) (6.1 g) was dissolved in a 1:1 mixture of dry DMF and dry pyridine, and mesyl chloride (0.5 mL; 6.5 mmol) was added. The solution was stirred over night at room temperature. The solvent was then removed under reduced pressure and the residue was dissolved in DMF. Subsequently, sodium azide (2.8 g; 43.2 mmol) was added, and the suspension was stirred for 2 days at 60 °C. The solution was then dialyzed against water for 5 days, with water change occurring twice a day, and the product was isolated by subsequent freeze-drying of the aqueous solution (4.0 g; 65.2%). The degree of intermediate functionalization was confirmed by ^{1}H-NMR spectroscopy of the mesylated compound, whereas ^{1}H-NMR of the resulting PHPMA-azide showed complete conversion of the mesyl groups, additionally supported by IR-spectroscopic detection of a band of azide vibration at ≈2100 cm^{-1}. PHPMA-mesylate: ^{1}H-NMR (400 MHz, DMSO-d$_6$, δ): 7.20 (b, -N*H*), 4.11 (m, -COO-C*H*$_2$-), 3.67 (m, -CH$_2$-C*H*OH-CH$_3$), 3.62 (b, -CH$_2$-C*H*$_2$-OH), 2.99 (m, -NH-C*H*$_2$-CHOH-), 2.33 (s, C*H*$_3$-SO$_2$), 2.00–0.68 (m, polymer backbone) ppm. PHPMA-azide: ^{1}H-NMR (400 MHz, DMSO-d$_6$, δ): 7.18 (b, -N*H*), 4.84 (m, -COO-C*H*$_2$-), 4.70 (m, -CH$_2$-C*H*OH-CH$_3$), 3.67 (m, -NH-C*H*$_2$-CHOH-), 3.54 (m, -CH$_2$-C*H*$_2$-N$_3$), 2.00–0.68 (m, polymer backbone) ppm. SEC (PEG calibration): M_n = 21,500 g mol^{-1}, M_w = 55,300 g mol^{-1}, M_w/M_n = 2.6.

Preparation of PNIPAAm: NIPAAm (5.0 g; 44.2 mmol) and 2-aminoethanethiol (AET) (68.2 mg; 0.6 mmol) were dissolved in dry DMF and the solution was preheated to 80 °C. AIBN (36.3 mg; 0.2 mmol) was added, and the solution was stirred at 80 °C over night. The product was obtained by precipitation achieved by pouring the solution into an excess of diethylether (4.3 g; 86.0%). With this approach, PNIPAAm could be prepared with a polystyrene-analog (apparent) number-average molecular weight of 10 000 g mol^{-1}. For a corresponding higher molecular mass of 25 000 g mol^{-1}, the amounts of AET (18.8 mg; 0.2 mmol) and AIBN (9.0 mg; 0.1 mmol) were adjusted as denoted in the parentheses. SEC (polystyrene calibration) (PNIPAAm$_{10,000}$): M_n = 10 300 g mol^{-1}, M_w = 35 600 g mol^{-1}, M_w/M_n = 3.5. SEC (polystyrene calibration) (PNIPAAm$_{25,000}$): M_n = 25 200 g mol^{-1}, M_w = 51 400 g mol^{-1}, M_w/M_n = 2.0.

Oscillatory Shear Rheology: Rheological studies were performed on a stress-controlled Anton Paar Physica MCR 301 rheometer with a parallel plate–plate geometry (gap size 1 mm, plate diameter 25 mm). For sample preparation, a semidilute solution of cyclooctyne-functionalized PNIPAAm and PEG in a mixture of water and cell medium (Dulbecco's Modified Eagles's Medium, pH 7.4) was evenly distributed in the middle of the lower plate at 28 °C, and the upper plate was lowered to evenly distribute the polymer solution on the upper geometry, too. The upper plate was then lifted again, a solution of azide-functionalized PHPMA in cell medium was added to the polymer solution on the lower plate, and the upper plate was lowered again. The overall polymer concentration was 100 g L^{-1}. For the first 90 min, each sample was monitored at a constant shearing amplitude and frequency (γ = 0.01; ω = 0.1 Hz) to ensure sample equilibration. Then, a frequency sweep was recorded at constant strain amplitude (γ = 0.01; ω = 0.01–16 Hz) at 28 °C. After increasing the temperature to 32 °C and allowing for equilibration for another 15 min, a second frequency sweep was recorded.

Microfluidic Emulsification and Microgel Fabrication: Microfluidic channels with four different inlets and a double cross-junction (Figure 3A) geometry were molded in poly(dimethylsiloxane) (PDMS) based soft lithography.[44] The microchannels had a rectangular cross-section with a uniform height of 180 µm. The channel width was 100 µm at the first cross-junction and 150 µm at the second crossjunction. A wide basin channel was patterned downstream of the second cross-junction to allow for observation of the resultant droplets, as illustrated in Figure 3B. All fluids were supplied to the microfluidic device using analytical plastic syringes and polyethylene tubing (Intramedic Clay Adams, Becton Dickinson, Sparks, MD 21152–0370, U.S.A.). The flow rates were adjusted by syringe pumps (Harvard Apparatus PhD Ultra). To monitor the droplet formation, the microfluidic device was operated on an inverted optical microscope (Zeiss Primo Vert) equipped with a digital camera (ABS UK1155). The different precursor polymer solutions were injected separately into two inlets (left and right on the microfluidic device), whereas the cells were injected into a third inlet (center), as illustrated in Figure 2A. At the first cross-junction, these three fluids formed a laminar coflowing stream in the microchannel, wherein which the cell suspension flowing in the middle served as a blocker for the reactive polymer precursors to meet and react. This stream was broken to form monodisperse pre-microgel droplets with diameters of 140 µm in the second cross-junction by flow focusing with immiscible low-viscous paraffin oil (94 wt%) containing a polyglycerol–polyricinoleate surfactant (PGPR 90, Danisco, Denmark, 6 wt%). Upon drop formation, mixing of the three aqueous liquids inside the droplets entailed rapid crosslinking of the precursor polymers by SPAAC in the presence of NIH 3T3 cells, thereby encapsulating them. The following volume flow rates were used for the PHPMA (51 g L^{-1}) and the mixture of functionalized PNIPAAm (167 g L^{-1}) and PEG (22 g L^{-1}) phases, the cell phase, and the continuous oil phase, respectively: 75:75:40:500 µL h^{-1}, resulting in microgels with a 100 g L^{-1} overall concentration. The resultant cell-laden microgel particles were transferred into cell medium by the following procedure: First, the supernatant organic phase was removed with a pipette. Then, the remaining sediment-microgels were suspended in cell medium, densified by centrifugation at 900 RCF, and then resuspended in fresh cell medium (pH 7.4); this procedure was repeated five times.

Supporting Information

Supporting Information is available from the Wiley Online Library or from the author.

Acknowledgements

This work was carried out at FU Berlin and Helmholtz-Zentrum Berlin, arced by the Berlin Joint Lab for Supramolecular Polymer Systems and supported by the Focus Area NanoScale and the Center for Research Strategy at FU Berlin; stem-cell encapsulation experiments were performed at Harvard University, supported by the NSF (DMR-1310266) and the Harvard MRSEC (DMR-1420570). D. S. is a research fellow of the Alexander von Humboldt Foundation. We thank Marlies Graewert (Max Planck Institute of Colloids and Interfaces, Golm) and Cathleen Schlesener (FU Berlin) for performing SEC analyses; we also thank Pia Keseberg and Jonas Schröder (both FU Berlin) for their help with part of the synthesis work as well as Junhua Xu (FU Berlin) for his help with part of the microgel swelling experiments. Furthermore, we thank Stefanie Wedepohl (FU Berlin) for providing NIH 3T3 cells.

Received: May 11, 2015
Published online: June 18, 2015

[1] M. A. C. Stuart, W. T. S. Huck, J. Genzer, M. Muller, C. Ober, M. Stamm, G. B. Sukhorukov, I. Szleifer, V. V. Tsukruk, M. Urban,

F. Winnik, S. Zauscher, I. Luzinov, S. Minko, *Nat. Mater.* **2010**, *9*, 101.
[2] G. Pellegrini, P. Rama, A. Rocco, A. Panaras, M. Luca, *Stem Cells* **2014**, *32*, 26.
[3] K. Y. Lee, D. J. Mooney, *Chem. Rev.* **2001**, *101*, 1869.
[4] L. G. Griffith, G. Naughton, *Science* **2002**, *295*, 1009.
[5] S. J. Lee, A. Atala, *Biomed. Mater.* **2013**, *8*, 010201.
[6] D. G. Seifu, A. Purnama, K. Mequanint, D. Mantovani, *Nat. Rev. Cardiol.* **2013**, *10*, 410.
[7] M. W. Tibbitt, K. S. Anseth, *Biotechnol. Bioeng.* **2009**, *103*, 655.
[8] E. Ruoslahti, J. C. Reed, *Cell* **1994**, *77*, 477.
[9] J. Meredith, B. Fazeli, M. Schwartz, *Mol. Biol. Cell.* **1993**, *4*, 953.
[10] M. Lutolf, J. Hubbell, *Nat. Biotechnol.* **2005**, *23*, 47.
[11] F. Guilak, D. M. Cohen, B. T. Estes, J. M. Gimble, W. Liedtke, C. S. Chen, *Cell Stem Cell* **2009**, *5*, 17.
[12] C. J. Flaim, S. Chien, S. N. Bhatia, *Nat. Methods* **2005**, *2*, 119.
[13] A. M. Kloxin, A. M. Kasko, C. N. Salinas, K. S. Anseth, *Science* **2009**, *324*, 59.
[14] S. Khetan, M. Guvendiren, W. R. Legant, D. M. Cohen, C. S. Chen, J. A. Burdick, *Nat. Mater.* **2013**, *12*, 458.
[15] R. Yoshida, K. Uchida, Y. Kaneko, K. Sakai, A. Kikuchi, Y. Sakurai, T. Okano, *Nature* **1995**, *374*, 240.
[16] J. Zhang, R. Xie, S.-B. Zhang, C.-J. Cheng, X.-J. Ju, L.-Y. Chu, *Polymer* **2009**, *50*, 2516.
[17] V. Aseyev, H. Tenhu, F. M. Winnik, in *Self Organized Nanostructures of Amphiphilic Block Copolymers II*, Springer, **2011**, pp. 29.
[18] H. G. Schild, *Prog. Polym. Sci.* **1992**, *17*, 163.
[19] S. Hirotsu, Y. Hirokawa, T. Tanaka, *J. Chem. Phys.* **1987**, *87*, 1392.
[20] B. Hashmi, L. D. Zarzar, T. Mammoto, A. Mammoto, A. Jiang, J. Aizenberg, D. E. Ingber, *Adv. Mater.* **2014**, *26*, 3253.
[21] G. Poli, M. Parola, *Free Radic. Biol. Med.* **1997**, *22*, 287.
[22] M. F. Moreau, D. Chappard, M. Lesourd, J. P. Monthéard, M. F. Baslé, *J. Biomed. Mater. Res.* **1998**, *40*, 124.
[23] G. Orive, R. M. Hernández, A. R. Gascón, R. Calafiore, T. M. Chang, P. De Vos, G. Hortelano, D. Hunkeler, I. Lacík, A. J. Shapiro, *Nat. Med.* **2003**, *9*, 104.
[24] A. Khademhosseini, R. Langer, J. Borenstein, J. P. Vacanti, *Proc. Natl. Acad. Sci. U.S.A.* **2006**, *103*, 2480.
[25] T. Rossow, J. A. Heyman, A. J. Ehrlicher, A. Langhoff, D. A. Weitz, R. Haag, S. Seiffert, *J. Am. Chem. Soc.* **2012**, *134*, 4983.
[26] D. Steinhilber, T. Rossow, S. Wedepohl, F. Paulus, S. Seiffert, R. Haag, *Angew. Chem. Int. Ed.* **2013**, *52*, 13538.
[27] J. D. Humphrey, E. R. Dufresne, M. A. Schwartz, *Nat. Rev. Mol. Cell. Biol.* **2014**, *15*, 802.
[28] J. Dommerholt, S. Schmidt, R. Temming, L. J. A. Hendriks, F. P. J. T. Rutjes, J. C. M. van Hest, D. J. Lefeber, P. Friedl, F. L. van Delft, *Angew. Chem. Int. Ed.* **2010**, *49*, 9422.
[29] S. Seiffert, W. Oppermann, *Macromol. Chem. Phys.* **2007**, *208*, 1744.
[30] S. Hackelbusch, T. Rossow, H. Becker, S. Seiffert, *Macromolecules* **2014**, *47*, 4028.
[31] A. Guiseppi-Elie, C. Dong, C. Z. Dinu, *J. Mater. Chem.* **2012**, *22*, 19529.
[32] O. Z. Fisher, N. A. Peppas, *Macromolecules* **2009**, *42*, 3391.
[33] T. Rossow, S. Bayer, R. Albrecht, C. C. Tzschucke, S. Seiffert, *Macromol. Rapid Commun.* **2013**, *34*, 1401.
[34] M. Y. Tang, J. E. Mark, *Macromolecules* **1984**, *17*, 2616.
[35] J. R. Falender, G. S. Y. Yeh, J. E. Mark, *J. Am. Chem. Soc.* **1979**, *101*, 7353.
[36] B. R. Dasgupta, D. A. Weitz, *Phys. Rev. E* **2005**, *71*, 021504.
[37] T. G. Mason, D. A. Weitz, *Phys. Rev. Lett.* **1995**, *74*, 1250.
[38] A. Habicht, W. Schmolke, F. Lange, K. Saalwächter, S. Seiffert, *Macromol. Chem. Phys.* **2014**, *215*, 1116.
[39] S. Seiffert, D. A. Weitz, *Soft Matter* **2010**, *6*, 3184.
[40] J. Nie, B. Du, W. Oppermann, *Macromolecules* **2005**, *38*, 5729.
[41] P. Debye, A. Bueche, *J. Appl. Phys.* **1949**, *20*, 518.
[42] M. Shibayama, *Bull. Chem. Soc. Jpn.* **2006**, *79*, 1799.
[43] R. Liu, W. Oppermann, *Macromolecules* **2006**, *39*, 4159.
[44] J. R. Anderson, D. T. Chiu, H. Wu, O. J. Schueller, G. M. Whitesides, *Electrophoresis* **2000**, *21*, 27.